

We are IntechOpen, the world's leading publisher of Open Access books Built by scientists, for scientists

4,800

Open access books available

122,000

International authors and editors

135M

Downloads

Our authors are among the

154

Countries delivered to

TOP 1%

most cited scientists

12.2%

Contributors from top 500 universities



WEB OF SCIENCE™

Selection of our books indexed in the Book Citation Index
in Web of Science™ Core Collection (BKCI)

Interested in publishing with us?
Contact book.department@intechopen.com

Numbers displayed above are based on latest data collected.

For more information visit www.intechopen.com



Automatic 3D Model Generation based on a Matching of Adaptive Control Points

Na-Young Lee¹, Joong-Jae Lee², Gye-Young Kim³ and Hyung-Il Choi⁴

¹Radioisotope Research Division, Korea Atomic Energy Research Institute

²Center for Cognitive Robotics Research, Korea Institute of Science and Technology

³School of Computing, Soongsil University

⁴School of Media, Soongsil University
Republic of Korea

Abstract

The use of a 3D model helps to diagnosis and accurately locate a disease where it is neither available, nor can be exactly measured in a 2D image. Therefore, highly accurate software for a 3D model of vessel is required for an accurate diagnosis of patients. We have generated standard vessel because the shape of the arterial is different for each individual vessel, where the standard vessel can be adjusted to suit individual vessel. In this paper, we propose a new approach for an automatic 3D model generation based on a matching of adaptive control points. The proposed method is carried out in three steps. First, standard and individual vessels are acquired. The standard vessel is acquired by a 3D model projection, while the individual vessel of the first segmented vessel bifurcation is obtained. Second is matching the corresponding control points between the standard and individual vessels, where a set of control and corner points are automatically extracted using the Harris corner detector. If control points exist between corner points in an individual vessel, it is adaptively interpolated in the corresponding standard vessel which is proportional to the distance ratio. And then, the control points of corresponding individual vessel match with those control points of standard vessel. Finally, we apply warping on the standard vessel to suit the individual vessel using the TPS (Thin Plate Spline) interpolation function. For experiments, we used angiograms of various patients from a coronary angiography in Sanggye Paik Hospital.

Keywords: Coronary angiography, adaptive control point, standard vessel, individual vessel, vessel warping.

1. Introduction

X-ray angiography is the most frequently used imaging modality to diagnose coronary artery diseases and to assess their severity. Traditionally, this assessment is performed directly from the angiograms, and thus, can suffer from viewpoint orientation dependence and lack of precision of quantitative measures due to magnification factor uncertainty

(Messenger et al., 2000), (Lee et al., 2006) and (Lee et al., 2007). 3D model is provided to display the morphology of vessel malformations such as stenoses, arteriovenous malformations and aneurysms (Holger et al., 2005). Consequently, accurate software for a 3D model of a coronary tree is required for an accurate diagnosis of patients. It could lead to a fast diagnosis and make it more accurate in an ambiguous condition.

In this paper, we present an automatic 3D model generation based on a matching of adaptive control points. Fig. 1 shows the overall flow of the proposed method for the 3D modelling of the individual vessel. The proposed method is composed as the following three steps: image acquisition, matching of the adaptive control points and the vessel warping. In Section 2, the acquisitions of the input image in standard and individual vessels are described. Section 3 presents the matching of the corresponding control points between the standard and individual vessels. Section 4 describes the 3D modelling of the individual vessel which is performed through a vessel warping with the corresponding control points. Experimental results of the vessel transformation are given in Section 5. Finally, we present the conclusion in Section 6.

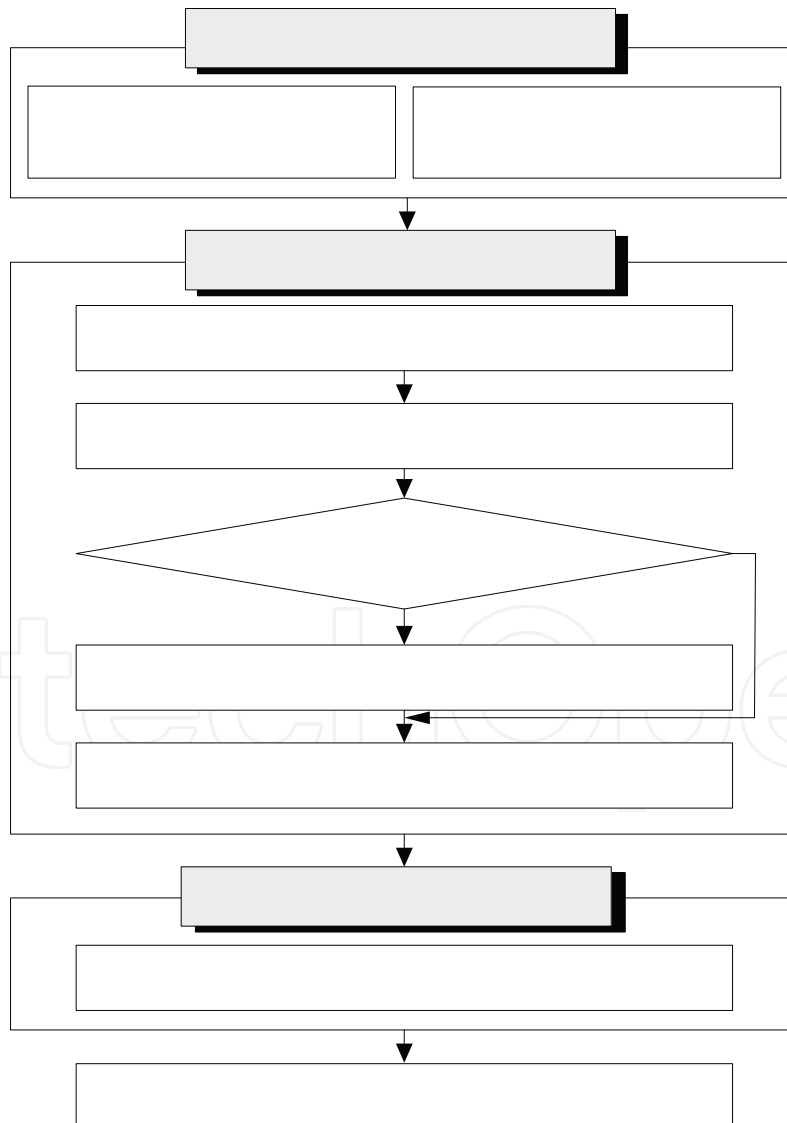


Fig. 1. Overall flow of the system configuration

2. Image Acquisition

We have generated a standard vessel because the shape of the arterial is different for each individual vessel, where the standard vessel can be adjusted to suit the individual vessel (Chalopin et al., 2001), (Lee et al., 2006) and (Lee et al., 2007). The proposed approach is based on a 3D model of standard vessel which is built from a database that implemented a Korean vascular system (Lee et al., 2006).

We have limited the scope of the main arteries for the 3D model of the standard vessel as depicted in Fig. 2.

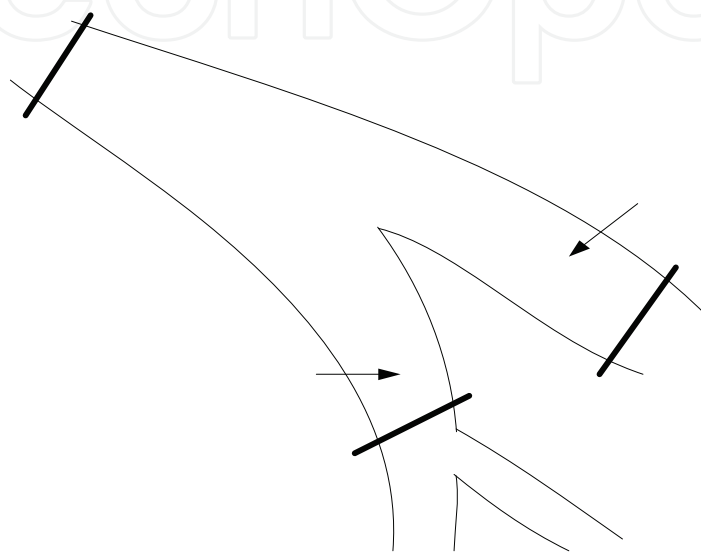


Fig. 2. Vessel scope of the database for the 3D model of the standard vessel

Table 1 shows the database of the coronary artery of Lt. main (Left Main Coronary Artery), LAD (Left Anterior Descending) and LCX (Left Circumflex artery) information. This database consists of 40 people with mixed gender information.

	age	Lt. main			LAD			LCX		
		Os	distal	length	Os	distal	length	Os	distal	length
below 60 years of old (male)	48.4±5.9	4.3±0.4	4.1±0.5	9.9±4.2	3.8±0.4	3.6±0.4	17.0±5.2	3.5±0.4	3.3±0.3	19.2±6.1
above 60 years of old (male)	67.5±5.4	4.5±0.5	4.4±0.4	8.4±3.8	3.9±0.3	3.6±0.3	17.2±5.8	3.6±0.4	3.4±0.4	24.6±8.9
below 60 years of old (female)	44.9±19.9	3.7±1.8	3.4±1.6	10.6±6.2	3.3±1.5	3.1±1.4	14.1±5.5	2.9±1.3	2.8±1.2	21.3±9.2
above 60 years of old (female)	70.7±4.4	4.3±0.7	4.1±0.6	12.5±7.9	3.5±0.6	3.4±0.5	22.3±7.3	3.3±0.4	3.1±0.3	27.5±3.7

Table 1. Database of the coronary artery

**Left Main
Coronary Artery**

To quantify the 3D model of the coronary artery, the angles of the vessel bifurcation are measured with references to LCX, Lt. main and LAD, as in Table 2. Ten individuals regardless of their gender and age were selected randomly for measuring the angles of the vessel bifurcation from six angiograms. The measurement results, and the average and standard deviations of each individual measurement are shown in Table 2.

	RAO30° CAUD30°	RAO30° CRA30°	AP0° CRA30°	LAO60° CRA30°	LAO60° CAUD30°	AP0° CAUD30°
1	69.17	123.31	38.64	61.32	84.01	50.98
2	53.58	72.02	23.80	51.75	99.73	73.92
3	77.28	97.70	21.20	57.72	100.71	71.33
4	94.12	24.67	22.38	81.99	75.6	69.57
5	64.12	33.25	31.24	40.97	135.00	61.87
6	55.34	51.27	41.8	80.89	119.84	57.14
7	71.93	79.32	50.92	87.72	114.71	58.22
8	67.70	59.14	31.84	58.93	92.36	70.16
9	85.98	60.85	35.77	54.45	118.80	78.93
10	47.39	60.26	34.50	47.39	67.52	34.79
Average	68.67	66.18	33.21	62.31	100.83	62.69
Standard deviation	14.56	29.07	9.32	15.86	21.46	13.06

Table 2. Measured angles of the vessel bifurcation from six angiographies

Fig. 3 illustrates the results of the 3D model generation of the standard vessel from six angiographies: RAO (Right Anterior Oblique)30° CAUD (Caudal)30°, RAO30° CRA (Cranial Anterior)30°, AP (Anterior Posterior)0° CRA (Cranial Anterior)30°, LAO (Left Anterior Oblique)60° CRA30°, LAO60° CAUD30°, AP0° CAUD30°.

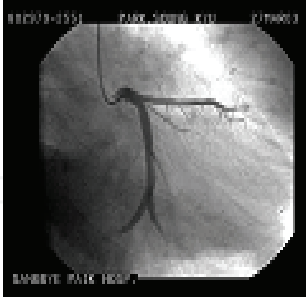
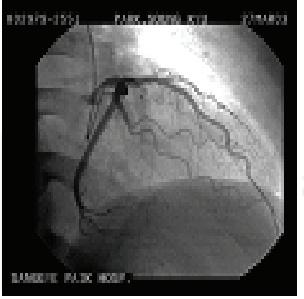
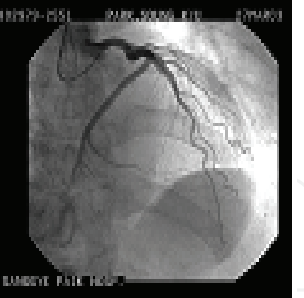

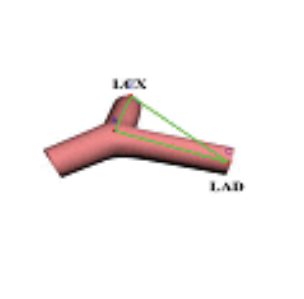
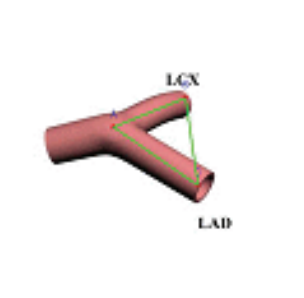
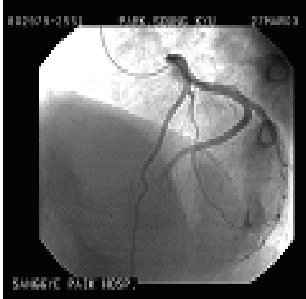
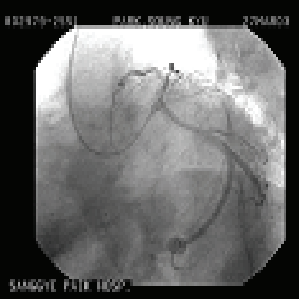
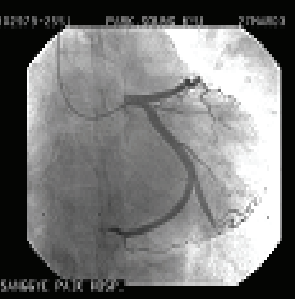
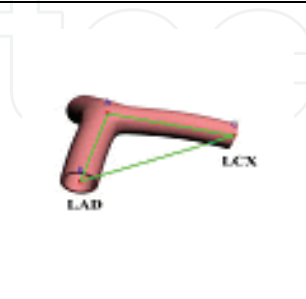

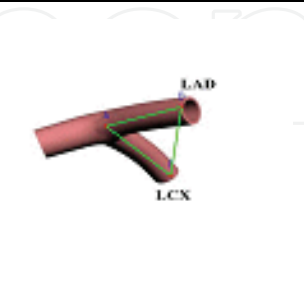
View	RAO30° CAUD30°	RAO30° CRA30°	AP0° CRA30°
Angiogram			
3D Model			
View	LAO60° CRA30°	LAO60° CAUD30°	AP0° CAUD30°
Angiogram			
3D Model			

Fig. 3. 3D model generation of the standard vessel from six angiographies

Evaluating the angles of the vessel bifurcation from six angiographies can reduce the possible measurement error which occurs when the angle from a single view is measured.

It is difficult to transform the standard vessel into individual vessel in a 3D space (Lee et al., 2006) and (Lee et al., 2007). Therefore, we projected the 3D model of the standard vessel into 2D projection. Fig. 4 shows the projected images of the standard vessel on a 2D plane through the projection. The projection result can be view as vertices or polygons based.

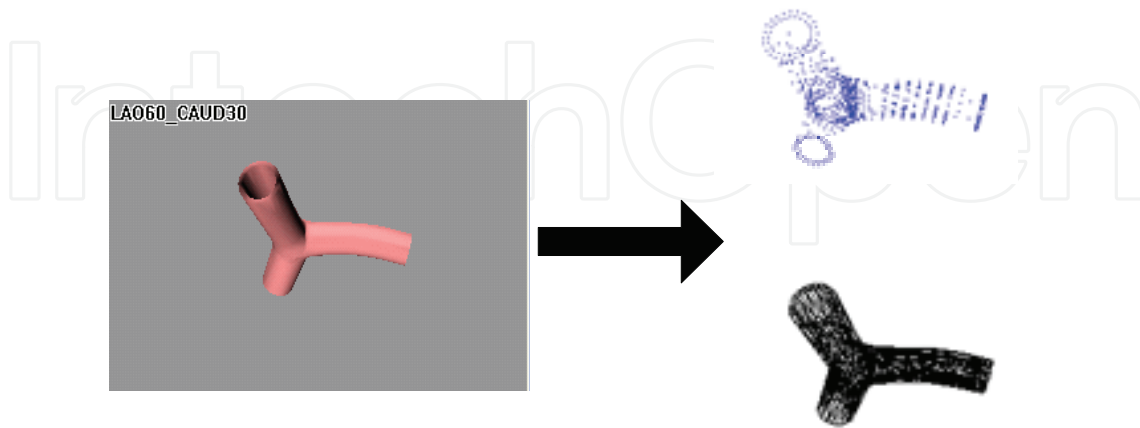


Fig. 4. Projection result for 2D image of standard vessel

3. Matching of the Adaptive Control Points

To transform a standard vessel into an individual vessel, it is important to match corresponding control points (Lee et al., 2006) and (Lee et al., 2007). In this paper, we extracted feature points of the vessel automatically and defined as control points (Lee et al., 2006) and (Lee et al., 2007). Feature points mean is referred to the corner points of an object or points with higher variance brightness compared to the surrounding pixels in an image, which are differentiated from other points in an image. Such feature points can be defined in many different ways in (Parker, 1996) and (Pitas, 2000). They are sometimes defined as points that have a high gradient in different directions, or as points that have properties that do not change in spite of specific transformations. Generally feature points can be divided into three categories (Cizek et al., 2004). The first one uses a non-linear filter, such as the SUSAN corner detector proposed by Smith (Woods et al., 1993) which relates each pixel to an area centered by a pixel. In this area, it is called the SUSAN area; all the pixels have similar intensities as the center pixel. If the center pixel is a feature point (some times a feature point is also referred to as a "corner"), SUSAN area is the smallest one among the pixels around it. A SUSAN corner detector can suppress a noise effectively without derivating an image. The second one is based on a curvature, such as the Kitchen and Rosenfeld's method (Maes et al., 1997). This kind of method needs to extract edges in advance, and then elucidate the feature points using the information on the curvature of the edges. The disadvantage of this method is required more needs a complicated computation, e.g. curve on fitting, thus its processing speed is relatively slow. The third method is exploits a change of the pixel intensity. A typical one is the Harris and Stephens' method (Pluim et al., 2003). It produces a corner response through an eigenvalues analysis. Since it does not need to use a slide window explicitly, its processing speed is very fast. Accordingly, this

paper used the Harris corner detector to find the control points of standard and individual vessels (Lee et al., 2006) and (Lee, 2007).

3.1 Extraction of the Control Points

The Harris corner detector is a popular interest point detector due to its strong invariance such as rotation, scale, illumination variation and image noise (Schmid et al., 2000) and (Derpanis, 2004). It is based on the local auto-correlation function of a signal. The local auto-correlation function measures the local changes of the signal with patches shifted by a small amount in different directions (Derpanis, 2004). However, the Harris corner detector has a problem where it can mistake those non-corner points.

Fig. 5 shows extracted 9 control points in individual vessel by using the Harris corner detector. We noticed that some of the extracted control points are non-corner points. To solve this problem of the Harris corner detector, we extracted more control points of individual vessel than standard vessel. Fig. 6 shows the extraction of control points from individual and standard vessels.

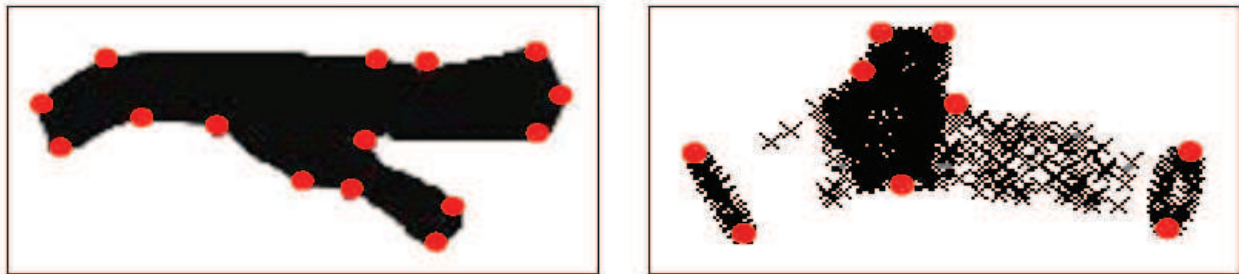


Fig. 5. Extracted 9 control points in individual vessel

3.2 Extraction of Corner Points

We performed thinning by using the structural characteristics of vessel to find the corner points among the control points of individual vessel which is extracted with the Harris corner detector (Lee, 2007). Fig. 7 shows the thinning process for detection of corner points in individual vessel.

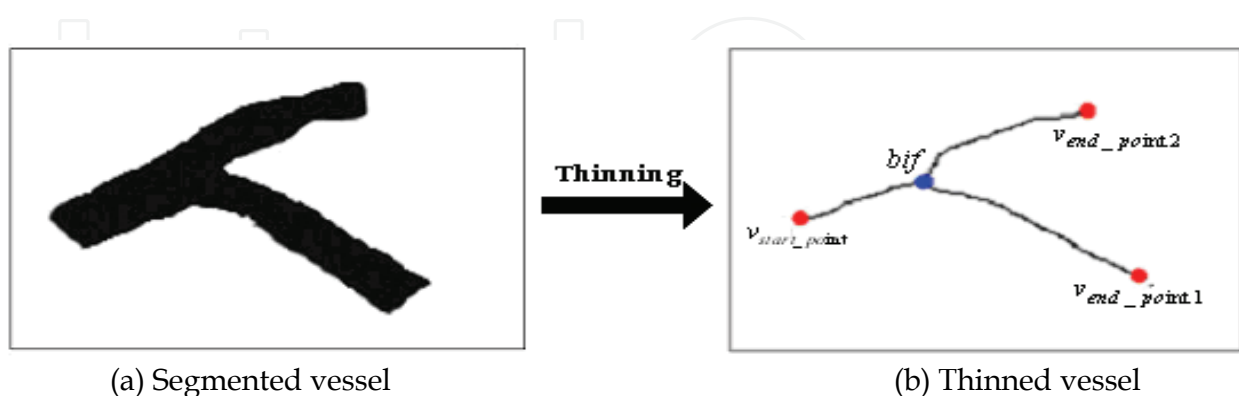


Fig. 6. Thinning process for detection of corner points in individual vessel

A vascular tree can be divided into a set of elementary components, or primitives, which are the vascular segments, and bifurcation (Wahle et al., 1994). Using this intuitive

representation, it is natural to describe the coronary tree by a graph structure (Chalopin et al., 2001) and (Lee, 2007).

A vascular tree of thinned vessel consists of three vertices (v_{point}) and one bifurcation (bif) as the following equation (1). Here, vertices (v_{point}) are comprised a start point (v_{start_point}) and two end points (v_{end_point1} , v_{end_point2}).

$$I_{thin} = \{ v_{point}, bif \} \quad (1)$$

$$v_{point} = \{ v_{start_point}, v_{end_point1}, v_{end_point2} \}$$

If the reference point is a vertex, the closest two control points to the vertex are defined as the corner points. If the reference point is a bifurcation, the three control points that are closest to it after comparing the distances between the bifurcation and all control points are defined as the corner points. As shown in Fig. 7, if the reference point is the vertex (v_{start_point}), v_1 and v_2 become the corner points; if the reference point is the bifurcation (bif), v_6 , v_{11} and v_{15} become the corner points (Lee, 2007).

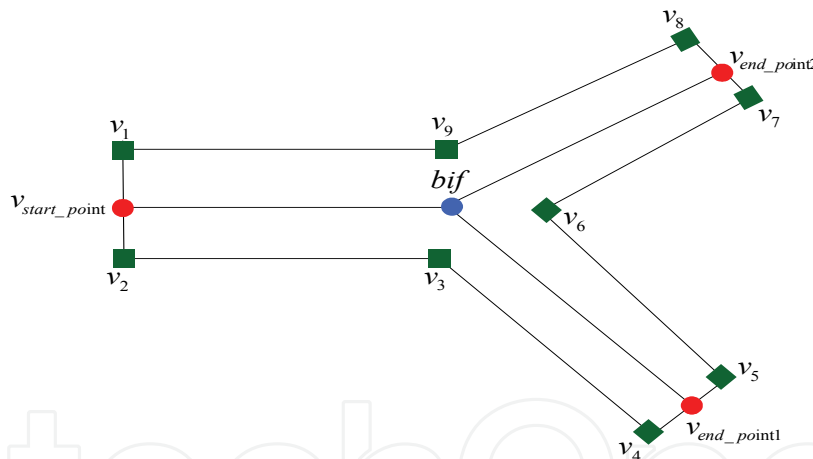


Fig. 7. Primitives of a vascular net

3.3 Adaptive Interpolation of the Control Points between Corner Points

Once the control points and corner points are extracted from an individual vessel, an interpolation for a standard vessel is applied. For an accurate matching, the control points are adaptively interpolated into the corresponding standard vessel in proportion to the distance ratio if there are control points between the corner points in an individual vessel (Lee, 2007).

Fig. 8 shows the process of an interpolation of the control points. Control points of a standard vessel are adaptively interpolated by the distance rate between control point (v_3) and two corner points (v_2 , v_4) of an individual vessel. Fig. 8 (a) shows the extracted control

points from an individual vessel, and (b) shows an example of control point interpolated between a standard vessel and the corresponding corner points from (a) image.

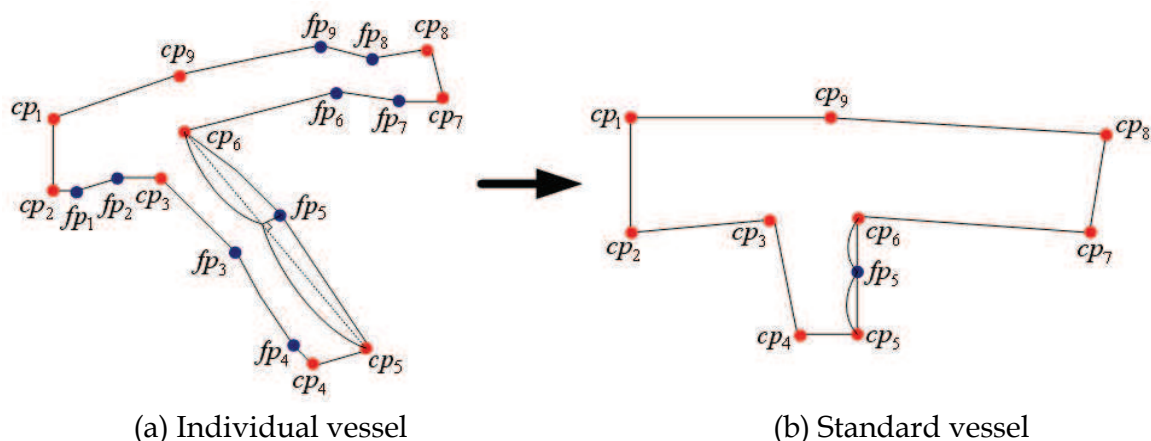


Fig. 8. Interpolation of the control points for a standard vessel

Fig. 9 shows the result of extracting the control points by using the Harris corner detector to the segmented vessel in the individual vessel and an adaptive interpolation of the corresponding the control points in the standard vessel.



Fig. 9. Result of an adaptive interpolation of the corresponding control points

4. Vessel Warping

We have warped the standard vessel with respect to the individual vessel. Given the two sets of corresponding control points, $S = \{s_1, s_2, \dots, s_m\}$ and $I = \{i_1, i_2, \dots, i_m\}$, the warping is applied the standard vessel to suit the individual vessel. Here, S is a set of control points in the standard vessel and I is a set of one in the individual vessel (Lee et al., 2006) and (Lee et al., 2007).

Standard vessel warping was performed using the TPS (Thin-Plate-Spline) algorithm (Bentoutou et al., 2002) from the two sets of control points.

The TPS is the interpolation functions that exactly represent a distortion at each feature point, and for defining a minimum curvature surface between control points. A TPS function is a flexible transformation that allows for a rotation, translation, scaling, and skewing. It also allows for lines to bend according by the TPS model (Bentoutou et al., 2002). Therefore, a large number of deformations can be characterized by the TPS model.

The TPS interpolation function can be written as equation (2).

$$h(x) = Ax + t + \sum_{i=1}^m W_i K(\|x - x_i\|) \quad (2)$$

The variables A and t are the affine transformation parameters matrices, W_i are the weights of the non-linear radial interpolation function K , and x_i are the control points. The function $K(r)$ is the solution of the biharmonic equation ($\Delta^2 K = 0$) that satisfies the condition of a bending energy minimization, namely $K(r) = r^2 \log(r^2)$.

The complete set of parameters, the interpolating registration transformation is defined, and then it is used to transform the standard vessel. It should be noted that in order to be able to carry out the warping of the standard vessel with respect to the individual vessel, it is required to have a complete description of the TPS interpolation function (Lee et al., 2006) and (Lee et al., 2007).

Fig. 10 shows the results of modifying the standard vessel to suit the individual vessel.

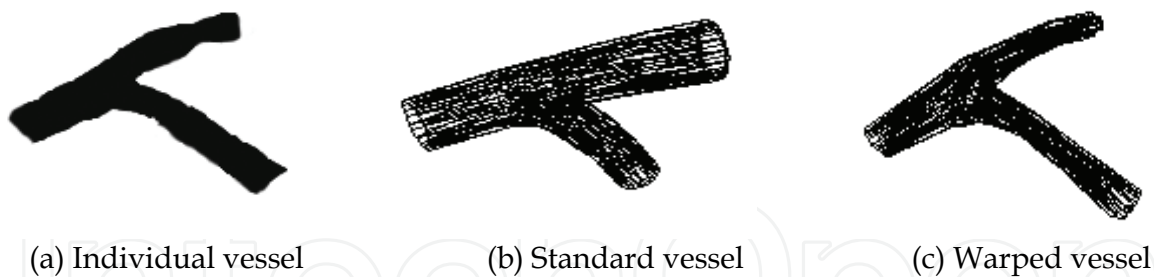


Fig. 10. Results of the warped vessel in standard vessel

5. Results of the Vessel Transformation

We simulated the system environment that is Microsoft Windows XP on a Pentium 3GHz, Intel Corp. and the compiler VC++ 6.0 is used. The image of 512× 512 is used for the experimentation. Each image has a gray-value resolution of 8 bits, i.e., 256 gray levels.

Fig. 11 shows the 3D model of the standard vessel from six different angiographic views. The results of the standard vessel warping using TPS algorithm to suit the individual vessel is shown in Fig. 13.

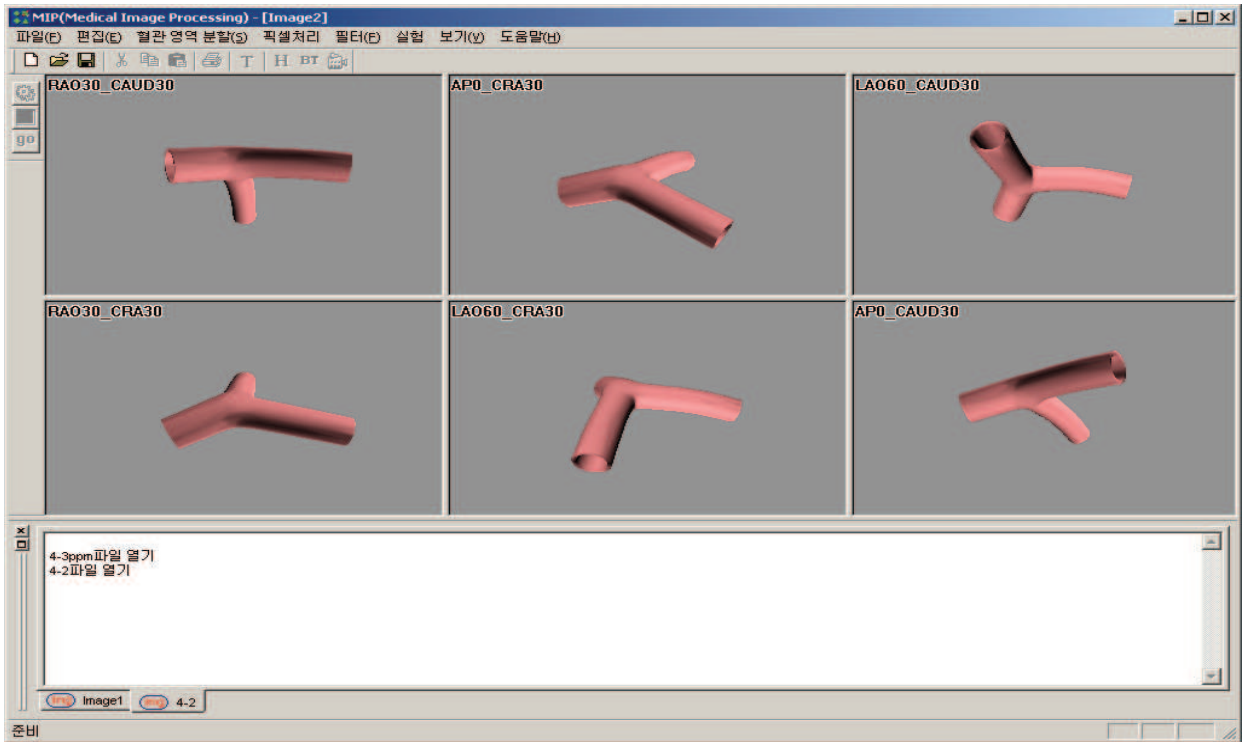


Fig. 11. 3D model of the standard vessel in angiographic of six different views

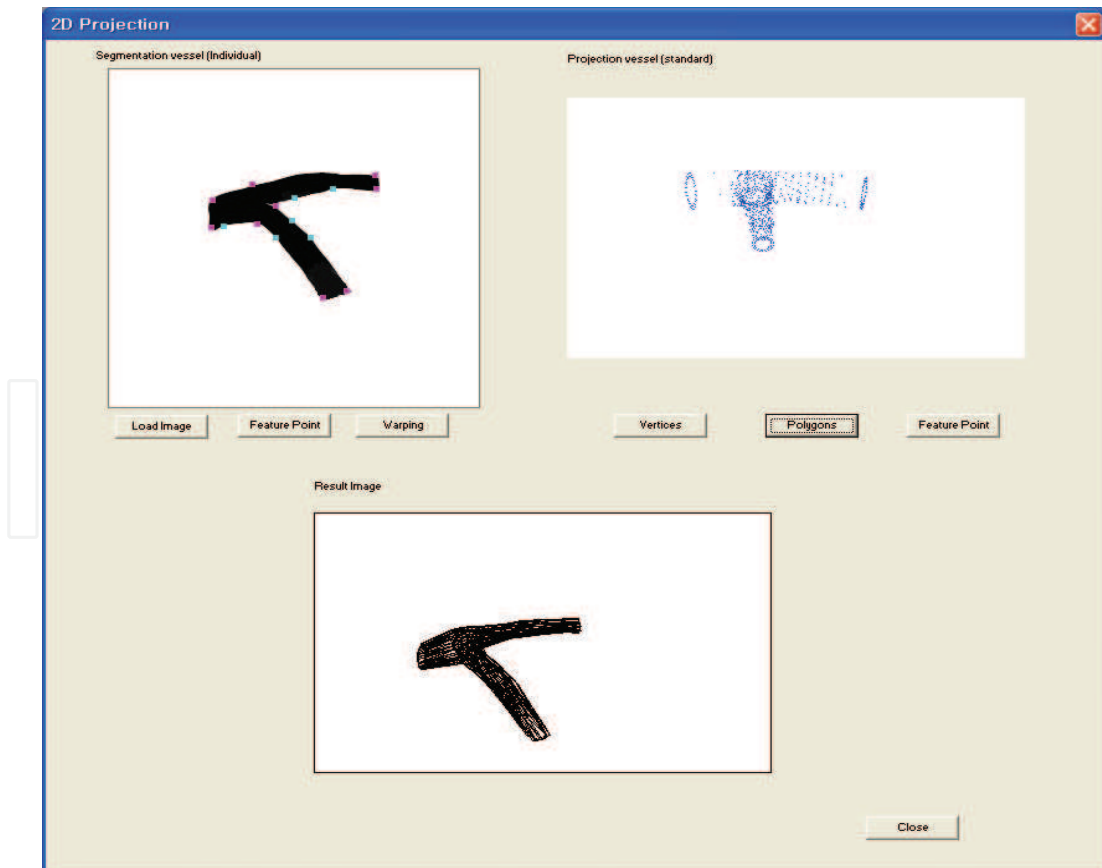


Fig. 12. Result of standard vessel warping

Fig. 13 shows the result for an automatically 3D model generation of individual vessel.

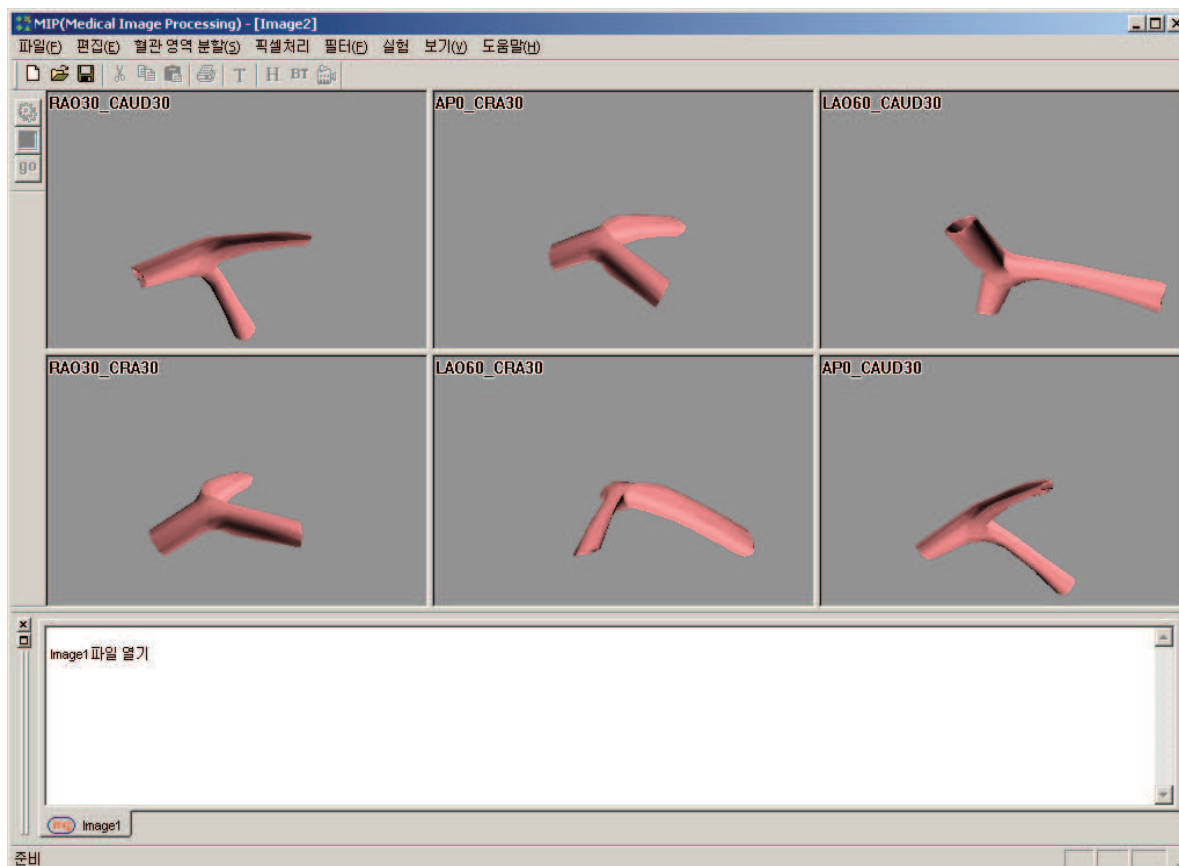


Fig. 13. Result of 3D model generation for the individual vessel in six views

6. Conclusion

We proposed a fully automatic and effective algorithm to perform a 3D modelling of individual vessel from angiograms in six views. This approach can be used to recover the geometry of the main arteries. The 3D model of the vessel enables patients to visualize their progress and improvement for a disease. Such a model should not only enhance the level of reliability but also provide a fast and accurate identification. In order words, this method can be expected to reduce the number of misdiagnosed cases (Lee et al., 2006) and (Lee et al., 2007).

7. Acknowledgement

“This Work was supported by Soongsil University and Korea Research Foundation Grant (KRF-2006-005-J03801) Funded by Korean Government.”

8. References

A, Venot.; J.F, Lebruchec. & J.C, Roucayrol. (1984). A new class of similarity measures for robust image registration, *Comput. Vision Graph. Image Process*, pp. 176-184.

- A, Wahle.; E, Wellnhofer.; I, Mugaragu.;H.U, Sauer.; H, Oswald. & E, Fleck. (1994). Accurate 3-D reconstruction and statistics for assessment of diffuse coronary artery disease, *Computers in Cardiology*, IEEE Computer Society, Los Alamitos, CA, pp.669-672
- B.G, Brown.; E, Bolson.; M, Frimer. & H, Dodge. (1977). Quantitative coronary arteriography estimation of dimensions, hemodynamic resistance, and atheroma mass of coronary artery lesions using the arteriogram and digital computation, *Circulation*, vol. 55, pp. 329-337
- C, Blondel.; R, Vaillant.; F, Devernary. ; G, Malandain. & N, Ayache. (2002). Automatic trinocular 3D reconstruction of coronary artery centerlines from rotational X-ray angiography, *Computer Assisted Radiology and Surgery 2002 Proceedings*, Paris, June 2002, Springer Publishers, Heidelberg
- Claire, Chalopin.; Gerard, Finet. & Isabelle E, Magnin. (2001). Modeling the 3D coronary tree for labeling purposes. *Medical Image Analysis*, pp.301-315
- Chris, Harris. & Mike, Stephens. (1988). A combined corner and edge detector, *Proceedings of the Fourth Alvey Vision Conference*, pp.147-151, Manchester
- C, Lorenz.; S, Renisch.; S, Schlatholter. & T, Bulow. (2003). Simultaneous Segmentation and Tree Reconstruction of the Coronary Arteries in MSCT Images, *Int. Symposium Medical Imaging, San Diego, Proc. SPIE Vol. 5032*, pp. 167-177
- C, Schmid.; R, Mohr. & C, Bauckhage. (2000). Evaluation of interest point detectors. *International Journal of Computer Vision*, pp. 151-172
- F.L, Bookstein. (1989). Principal warps: thin-plate splines and the decomposition of deformations, *IEEE-PAMI* 11, pp. 567-585
- F, Maes.; A, Collignon.; G, Marchal. & P, Suetens. (1997). Multimodality image registration by maximization of mutual information, *IEEE Transaction on Medical Imaging*, Vol. 16, No. 2, pp.187-198
- Holger, Schmitt.; Michael, Grass.; Rolf, Suurmond.; Thomas Kohler.; Volker, Rasche.; Stefan, Hahnel. & Sabine, Heiland. (2005). Reconstruction of blood propagation in three-dimensional rotational X-ray angiography. *Computerized Medical Imaging and Graphics*, 29, pp. 507-520
- I, Pitas. (2000). *Digital image processing algorithms and applications, 1st Ed.*, John Wiley & Sons, Inc., ISBN 0471377392, New York
- J.C, Messenger.; S.Y,Chen.; J.D, Carroll.; J.E, Burchenal.; K, Kioussopoulos. & B.M, Groves. (2000). 3D coronary reconstruction from routine single-plane coronary angiograms: clinical validation and quantitative analysis of the right coronary artery in 100 patients, *The International Journal of Cardiac Imaging* 16(6), pp.413-427
- J, Cizek.; K, Herholz.; S, Vollmar.; R, Schrader.; J, Klein. & W.D, Heiss. (2004). Fast and robust registration of PET and MR image of human brain, *Neuroimage*, Vol. 22, Iss. 1, pp.434-442
- J, Flusser. & T,Suk. (1998). Degraded image analysis: an invariant approach, *IEEE Trans. Pattern Anal. Mach. Intell.*, pp. 590-603
- Jianbo, Shi. & Carlo, Tomasi. (1994). Good features to track, *IEEE Conference on CVPR Seattle*, pp. 593-600
- J.P.W, Pluim.; J.B.A, Maintz. & M.A, Viergever. (2003). Mutual information based registration of medical images: a survey, *IEEE Transactions on Medical Imaging*, Vol. 22, No. 8, pp. 986-1004

- J.R, Parker. (1996). *Algorithms for image processing and computer vision, 1st Ed.*, John Wiley & Sons, Inc., ISBN 0471140562, USA
- J, Ross. et al. (1987). Guidelines for coronary angiography, *Circulation*, vol.76
- K, Derpanis. (2004). The Harris corner detector
- M, Grass.; R, Koppe.; E, Klotz.; R, Proksa.; MH, Kuhn.; H, Aerts. & etc (1999). 3D reconstruction of high contrast objects using C-arm image intensifier projection data, *Computer Med Imaging Graphics*, 23(6):311-321
- M, Grass.; R, Koppe.; E, Klotz.; Op de Beek J. & R, Kemkers. (1999). 3D reconstruction and imaging based on C-arm systems, *Med Biol Eng Comput*, 37(2):1520-1
- M, Grass.; R, Guillemaud.; R, Koppe.; E, Klotz.; V, Rasche. & Op de Beek J. (2002). *La radiologie tridimensionnelle, La tomography medicale-imagerie morphologique et imagerie fonctionnelle*, Hermes Science Publications, Paris
- Na-Young, Lee.; Gye-Young, Kim. & Hyung-Il, Choi. (2006). Automatic generation technique of three-dimensional model corresponding to individual vessels, *Computational Science and Its Applications-ICCSA 2006*, LNCS 3984, PP.441-449, Glasgow, UK, May 2006, Springer-Verlag Berlin Heidelberg
- Na-Young, Lee. (2006). An automatic generating technique of individual vessels based on general vessels, *The 7th International Workshop on Image Analysis for Multimedia Interactive Services*, pp.241-244, Korea, April, 2006, Incheon
- NaYoung, Lee.; JeongHee, Cha.; JinWook, On.; GyeYoung, Kim. & HyungIl, Choi. (2006). An automatic generation technique of 3D vessels model form angiograms, *Proceedings of The 2006 International Conference on Image Processing, Computer Vision, & Pattern Recognition*, pp.371-376, USA, June, 2006, CSREA Press, Las Vegas
- Na-Young, Lee. (2007). Automatic generation of 3D vessels model using vessels image matching based on adaptive control points, *Sixth International Conference on Advanced Language Processing and Web Information Technology*, pp.265-270, ISBN 0-7695-2930-5, China, August 2007, IEEE Computer Society, Luoyang, Henan
- Na-Young, Lee.; Gye-Young, Kim. & Hyung-Il, Choi. (2007). 3D modelling of the vessels from X-ray angiography, *Digital Human Modeling, HCII 2007*, LNCS 4561, pp.646-654, ISBN 978-3-540-73318-8, Springer Berlin Heidelberg
- Na-Young, Lee.; Gye-Young, Kim. & Hyung-Il, Choi. (2007). 3D model of vessels from angiograms, *Proceedings of the 13th Japan-Korea join workshop on frontiers of computer vision*, pp.235-240, Korea, January 2007, Busan
- Na-Young, Lee. (2007). Three Dimensional Modeling of Individual Vessels Based on Matching of Adaptive Control Points, *MICAI 2007: Advances in Artificial Intelligence*, LNAI 4827, pp. 1143-1150, Springer-Verlag Berlin Heidelberg
- P, de Feyter.; J, Vos.; J, Reiber. & P, Serruys. (1993). Value and limitations of quantitative coronary angiography to assess progression and regression of coronary atherosclerosis. *In Advances in Quantitative Coronary Arteriography*, pp. 255-271
- R.P, Woods.; J.C, Mazziotta. & S.R, Cherry. (1993). MRI-PET registration with automated algorithm, *Journal of computer assisted tomography*. Vol. 17:44, pp.536-546
- Y, Bentoutou.; N, Taleb.; M, Chikr El Mezouar, M, Taleb. & L, Jetto. (2002). An invariant approach for image registration in digital subtraction angiography. *Pattern Recognition*, Vol. 35, Iss. 12, December 2002, pp. 2853-2865



Adaptive Control

Edited by Kwanho You

ISBN 978-953-7619-47-3

Hard cover, 372 pages

Publisher InTech

Published online 01, January, 2009

Published in print edition January, 2009

Adaptive control has been a remarkable field for industrial and academic research since 1950s. Since more and more adaptive algorithms are applied in various control applications, it is becoming very important for practical implementation. As it can be confirmed from the increasing number of conferences and journals on adaptive control topics, it is certain that the adaptive control is a significant guidance for technology development. The authors the chapters in this book are professionals in their areas and their recent research results are presented in this book which will also provide new ideas for improved performance of various control application problems.

How to reference

In order to correctly reference this scholarly work, feel free to copy and paste the following:

Na-Young Lee, Joong-Jae Lee, Gye-Young Kim and Hyung-II Choi (2009). Automatic 3D Model Generation based on a Matching of Adaptive Control Points, Adaptive Control, Kwanho You (Ed.), ISBN: 978-953-7619-47-3, InTech, Available from:

http://www.intechopen.com/books/adaptive_control/automatic_3d_model_generation_based_on_a_matching_of_adaptive_control_points__

INTECH

open science | open minds

InTech Europe

University Campus STeP Ri
Slavka Krautzeka 83/A
51000 Rijeka, Croatia
Phone: +385 (51) 770 447
Fax: +385 (51) 686 166
www.intechopen.com

InTech China

Unit 405, Office Block, Hotel Equatorial Shanghai
No.65, Yan An Road (West), Shanghai, 200040, China
中国上海市延安西路65号上海国际贵都大饭店办公楼405单元
Phone: +86-21-62489820
Fax: +86-21-62489821

© 2009 The Author(s). Licensee IntechOpen. This chapter is distributed under the terms of the [Creative Commons Attribution-NonCommercial-ShareAlike-3.0 License](#), which permits use, distribution and reproduction for non-commercial purposes, provided the original is properly cited and derivative works building on this content are distributed under the same license.

IntechOpen

IntechOpen